Journal of Hydrology 643 (2024) 132025

Contents lists available at ScienceDirect

Journal of Hydrology

journal homepage: www.elsevier.com/locate/jhydrol

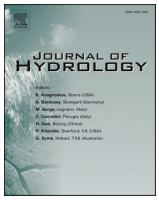

Research papers

Characterizing the Kamphorst rainfall simulator for soil erosion investigations

F.G. Carollo [a], R. Caruso [a], V. Ferro [a,b], M.A. Serio [a,*]

[a] Department of Agricultural, Food and Forest Sciences, University of Palermo, Palermo, Italy
[b] NBFC, National Biodiversity Future Center, 90133 Palermo, Italy

ARTICLE INFO

Keywords:
Rainfall simulation
Rainfall intensity
Rainfall kinetic power
Rainfall momentum

ABSTRACT

In this paper, the results of the characterization of Kamphorst's rainfall simulator obtained by laboratory experiments carried out at the Department of Agricultural, Food, and Forest Sciences of the University of Palermo, are presented. At first, the rainfall uniformity distribution was positively verified considering several pressure heads (ranging from 1.9 cm to 11.9 cm) and water temperatures (from 24 °C to 27 °C), achieving a uniformity coefficient ranging from 96 to 99 %. Then, using a single nozzle, the simulator has been characterized in terms of kinetic power and momentum by applying both a photographic and a weighing technique. In particular, terminal drop velocity was measured by the displacement of a single raindrop measured between two consecutive frames, while the mean mass of single drops was evaluated by weighing a fixed number of drops. The analysis of the experimental data highlighted that the rainfall intensity, which increases with water temperature and pressure head, is the variable affecting the measurement of the single raindrop mass. Measurements also showed that an increase in rainfall intensity determines a decrease in the mean mass of the raindrops and an increase in the number of raindrops that fall in the unit time and area. This circumstance allowed to justify the increasing trend of the rainfall kinetic power and momentum with rainfall intensity. The measurements allowed to develop empirical relationships relating kinetic power and momentum with the simulated rainfall intensity and falling height of the raindrops. Finally, a theoretical expression suggested in the literature for estimating simulated rainfall intensity was positively tested.

1. Introduction

Rainfall simulators are very attractive devices for investigating several hydrological and erosive processes, allow to control the characteristics of the agent responsible for runoff and erosion, and easily replicate the experiment under controlled conditions and over relatively short time periods. Small portable rainfall simulators have been used worldwide by different research groups for many years and, since 1938, more than 100 rainfall simulators with plot dimensions < 5 m^2 (most of them < 1 m^2) were developed (Neal, 1938; Wilm, 1943; Adams et al., 1957; Hudson, 1965; Bryan, 1974; Imeson, 1977; De Ploey, 1981; Luk, 1985; Roth et al., 1985; Farres, 1987; Kamphorst, 1987; Norton, 1987; Calvo et al., 1988; Poesen et al., 1990; Cerdà et al., 1997; Torri et al., 1999; Battany and Grismer, 2000; Regmi and Thompson, 2000; Loch et al., 2001; Martínez-Mena et al., 2001; Humphry et al., 2002; Blanquies et al., 2003; Regüés and Gallart, 2004; Birt et al., 2007; Clarke and Walsh, 2007; Alves Sobrinho et al., 2008; Nadal-Romero and Regüés, 2009; Abudi et al., 2012; Iserloh et al., 2013). Moreover, no standardization of rainfall simulation and test conditions makes it difficult to compare the results available in the literature (Lascelles et al., 2000; Clarke and Walsh, 2007; Boulal et al., 2011; Ries et al., 2013).

A summary of major requirements for small portable rainfall simulators is given in Iserloh et al. (2013). The authors studied and compared the performances of 13 different rainfall simulators placed in several European research institutions, from the perspective of rainfall intensity, drop size and energetic distribution. The authors also evaluated the rainfall uniformity distribution for all investigated rainfall simulators, except for the Kamphorst one, and the Christiansen Uniformity coefficient (*CU*) was calculated using the following equation (Christiansen 1942):

$$CU = \left(1 - \frac{\sum_{i=1}^{n} |I_i - I_S|}{I_S n}\right) \quad (1)$$

* Corresponding author.
E-mail address: mariaangela.serio@unipa.it (M.A. Serio).

https://doi.org/10.1016/j.jhydrol.2024.132025
Received 18 March 2024; Received in revised form 31 May 2024; Accepted 3 September 2024
Available online 16 September 2024

where $\sum_{i=1}^{n}|I_i - I_S|$ is the sum of the absolute deviations of the rainfall intensity I_i (mm h^{-1}) of a single nozzle from the mean rainfall intensity I_S (mm h^{-1}), and n is the total number of nozzles. Christiansen Uniformity coefficient values greater than 60 % have been registered. As reported by Iserloh et al. (2013) a CU>80 % is fundamental to guarantee the correct functioning and reproducibility of rainfall intensity simulation experiments.

It is well known that the main and critical properties of a simulated rainfall are its spatial distribution, the drop size distribution (DSD), the fall velocities of the drops, and the kinetic energy. These variables have been widely investigated for natural precipitation and, over the years, many empirical or theoretical relationships to estimate rainfall kinetic power, P_n (J m^{-2} s^{-1}), which is the kinetic energy per unit area and time, by other rainfall variables (rainfall intensity, shape and scale parameter of DSD), have been proposed in the literature (Carollo et al., 2017; Carollo et al., 2018a, b; Serio et al., 2019a, b).

To the best of our knowledge, no relationship to estimate P_n by simulated rainfall intensity, I_S (mm h^{-1}), has been suggested for the different simulators available in the literature.

To date, many techniques have been used to measure simulated rainfall DSD, such as the flour pellet method (Laws and Parsons, 1943; Hudson, 1963), laser particle measuring system (Salles and Poesen, 1999; Salles et al., 1999), plaster micro plot (Ries and Langer, 2001; Ries et al., 2009), indication paper (Wiesner, 1895; Brandt, 1989; Cerdà et al., 1997; Salles et al., 1999), Joss-Waldvogel Disdrometer (Joss and Waldvogel, 1967; Hassel and Richter, 1988; Bahddou et al, 2023), oil method (Gunn and Kinzer, 1949), and photographic method (Kavian et al., 2018; Etheridge, 2023; Kalehhouei et al., 2023).

Ries et al. (2009) characterized the rainfall produced by a rainfall simulator fed with a pressure of about 2 bar at a height of 2 m and a rainfall intensity value of 40 mm h^{-1} (Ries et al., 2000; Ries and Langer, 2001 Seeger, 2007). Four different calibration methods were used to assess the drop size distribution: Indication Paper, Plaster Micro Plot, Joss–Waldvogel Disdrometer, and Laser Distrometer (Thies). They suggested that the effectiveness of the results of the characterization of simulated rainfall was extremely dependent on the applied method. Ries et al. (2009) stated that the most inaccuracy occurred for drop fall velocity measurements. They indicated that small drops moved with "*an unrealistic high velocity*" and that an available height of 2 m is not sufficient for accelerating and reaching terminal velocity. Moreover, the high fall velocity of very small drops forbade the laser disdrometer from recognizing all raindrops. This circumstance also influenced the estimation of the total amount of precipitation, the average drop size, and the median volumetric drop diameter, which resulted to be smaller than the ones measured with other methods (e.g., Shelton et al. (1985), Lascano et al. (1997) Salles et al. (1999) and Humphry et al. (2002), Blanquies et al. (2003)).

Covert and Jordan (2009) analyzed simulated droplet size distributions by using a digital camera that captured drops on a grid screen. Droplet diameters less than or equal to 6 mm were measured. The authors also reported that rainfall simulators should be designed with nozzles at a height of 3 m at least in order to achieve the drop terminal velocity and simulate the kinetic energy of natural rainfall.

Abudi et al. (2012) applied a high frame-rate camera, capable of capturing 8000 frames per second, for monitoring the simulated falling drops (in the range of 1–5.2 mm) and calculating their size and velocity.

Sadeghi et al. (2013) recorded raindrops at several intensities in Mazandaran Province using a Canon EOS 550D camera capable of recording 4000 frames per second. To enhance the measurement accuracy, they omitted the droplets located out-of-focus of the camera lens. The measured droplet diameter ranged from 0.2 mm to 6 mm, and the measurements carried out by the photographic method were rather similar to those obtained by the flour method.

Cerdà et al. (1997) used the photographic technique to measure the speed of the drops and determined the size by other methods such as the flour one. They suggested that the raindrop size increases with the reduction of the nozzle water pressure and thus falls with a low-velocity value. In their investigation, the raindrop did not have adequate space to reach its terminal velocity.

A small device, easily transportable, that has been widely used up to the present day for soil conservation surveys, was developed at Wageningen Agricultural University and first described by Kamphorst (1987). The simulator has a sprinkler with 49 capillary tubes and a built-in pressure regulator based on Mariotte's bottle principle, that allows for maintaining constant the rainfall intensity value during the rainfall simulation.

The geometry of the sprinkling head characterized by 49 capillary tubes having a fixed position determines that drops flowing from a single tube impacts always at the same point during an experimental run.

The pressure head on the capillaries can be increased or decreased by moving an aeration tube upward or downward. According to Kamphorst (1987), this pressure head regulation is oriented to correct for the influence of the viscosity, which depends on water temperature. In fact, the device was not initially meant to be used to produce showers of different intensities but to obtain a standard rainshower. However, Bagarello et al. (1996) proved that rainfall intensity can be significantly changed by moving the aeration tube of this simulator and developed an empirical relationship between rainfall intensity, the position of the aeration tube, and water temperature T (°C). In particular, using this empirical relationship to I_S estimate and considering the volume of the Mariotte's bottle equal to 2.3 l, T=25 °C and the position of the aeration tube ranging from 0 cm to 10 cm, the Kamphorst simulator produces I_S values varying from 258 mm h^{-1}(8.6 min) to 864 mm h^{-1} (2.6 min).

For predicting rainfall intensity flowing out of Kamphorst's simulator capillaries, Agosta et al. (2022) developed a theoretical relationship based on the application of the Bernoulli theorem to the two cross-sections corresponding to the inlet (1) and the outlet (2) section of the capillary tube, the Poiseuille's law to calculate the head loss Y between the two sections, and considering the horizontal plane passing through the section 2 as the reference level:

$$i = \frac{16}{d^2}\frac{\mu}{\rho}\frac{l_u}{1-\frac{\alpha_1}{2}}\left[-1+\sqrt{1+\frac{g\left(1-\frac{\alpha_1}{2}\right)(H+l_u)}{\left(\frac{16}{d^2}\frac{\mu}{\rho}l_u\right)^2}}\right] \quad (2)$$

where d (m) and l_u (m) are, respectively, the diameter and length of the capillary tube, H (m) is the pressure head, μ (kg s/m^{-2}(−|-)) is the water viscosity, ρ (kg m^{-3}) is the water density, and α_1 is the Coriolis coefficient at section 1. In other words, according to Eq. (2) the physical properties of the fluid (μ, which depends on the water temperature, and ρ) and the geometric characteristics of the capillary tube, affect the calculation of i, and the Coriolis coefficient α_1 is the only parameter that must be estimated by fitting Eq. (2) to measurements. Rainfall intensity per unit time and area, I_s (mm h^{-1}), can be calculated by Eq. (2):

$$I_s = i\frac{\pi d^2}{4}\frac{n_c}{\sigma} \quad (3)$$

where n_c is the number of capillaries and σ (m^2) is the surface area of the test plot, which are respectively equal to 49 and 0.0625 m^2 for the Kamphorst simulator.

Agosta et al. (2022) positively tested Eq. (2) to reproduce the i measurements carried out using the Kamphorst simulator, established that the reliability of Eq. (2) is independent of the considered pressure head and water temperature and these measurements of i yielded to α_1 = 1.25.

Iserloh et al. (2013) energetically characterized the Kamphorst simulator using raindrop size distribution and falling velocity measurements carried out with the Thies Laser Precipitation Monitor. For this rainfall simulator, the authors found that kinetic power values are

greater than those calculated for natural rainfall. Iserloh et al. (2013) justified this because the Kamphorst simulation is characterized by a very short test duration, and it also produces large and high-energy drops.

The aim of this investigation is the characterization of the Kamphorst simulator for different pressure head and water temperature values, giving operative information about its functioning, uniformity of rainfall intensity distribution, and the amount of kinetic power and momentum that rainfall discharges into the soil. New empirical relationships to estimate the kinetic power and momentum by simulated rainfall intensity and falling height are also proposed.

2. Material and methods

2.1. Experimental set-up

The experimental setup (Fig. 1), placed in the laboratory of the Department of Agricultural, Food, and Forest Sciences of the University of Palermo (Italy), consists of a Kamphorst rainfall simulator (model type 09.06) (Eijkelkamp, 2022) (Fig. 2), placed inside a wooden support positioned above a metal structure (1.9 m high and 1.2 m wide). The installation is also equipped with a stopwatch, a scale (model MP-3000G, made by Chyo), a foldable metal ladder, a tank for water storage, a mobile phone camera, and an opaque color background panel. The frame rate of the camera, which records slow motion video at 720p resolution, is 480 FPS (Frame Per Second). The mobile phone is supported and leveled by a vertically extendable photographic tripod, allowing to position camera lenses in parallel with the falling direction of the simulated rain. Since the minimum height at which the camera can be positioned above the photographic tripod is 60 cm, the maximum explorable falling height, for the considered experimental setup, is equal to 1.3 m. A meter ruler was also placed in parallel with the falling direction of the drops to calculate the distance traveled by a raindrop during its fall. During the recordings, the distance between the camera lenses and the ruler was 24 cm. A led lamp, opposite the camera and 40 cm behind the background panel, was also used to guarantee raindrop recognition in the frames. A collector system (Fig. 3) was also built to evaluate the rainfall intensity spatial uniformity. It is constituted of 49 Falcon® 50 ml PP conical tubes housed on a polystyrene structure according to the nozzle scheme of the simulator plate.

2.2. Procedure to verify the rainfall intensity uniformity distribution of the simulator

In the Kamphorst simulator, the sprinkling head is connected to a cylindrical reservoir having a capacity of almost 2.3 l (Kamphorst, 1987; Bagarello and Ferro, 2004) (Fig. 2).

At the base of the sprinkling head, there is a plate in which 49 glass capillaries are positioned. Each capillary tube is 10 ± 1 mm long and has a diameter of 0.6 ± 0.08 mm.

Removing (or positioning) the cap on the top of the aeration tube determines the starting (stopping) of water flow from the capillaries, while the moving of the aeration tube upward or downward provokes a change of the pressure head, H, on the capillaries' inlet section, which determines different values of simulated rainfall intensity, I_S. This simulator allows to set H ranging from 1.9 cm to 11.9 cm. For small values of H ($\leq$5cm), the simulation was stopped when the water level reached the plane passing through the bottom of the cylindrical reservoir of the sprinkler since the lower edge of the aeration tube was deeper as compared with this plane. Instead, for $5 < H \leq 12$ cm, the simulation was stopped when the water level reached the plane passing through the lower edge of the aeration tube. In this way, the pressure head on the orifices did not change during a simulation.

To evaluate the rainfall intensity uniformity distribution of the Kamphorst simulator, tests were carried out using water temperature T varying from 24 °C to 27 °C, and H value ranging from 1.9 to 11.9 cm.

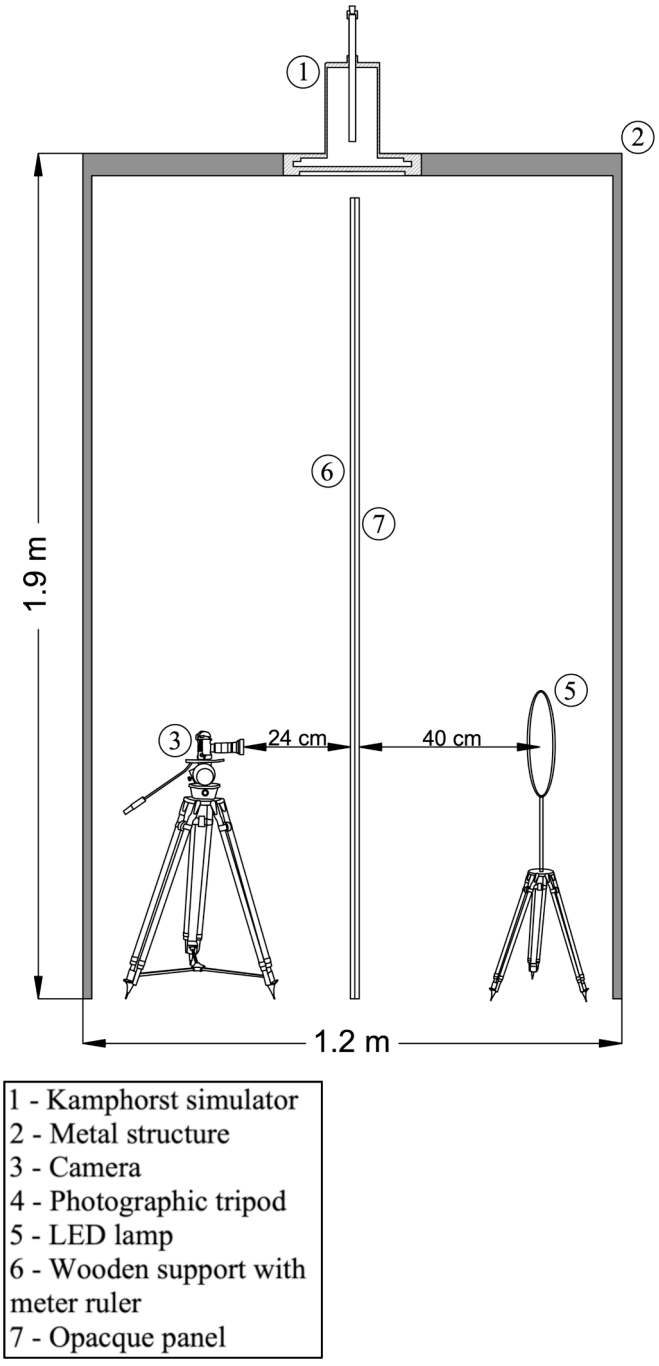

Fig. 1. Scheme of the experimental layout.

Placing the collector system (Fig. 3) under the rainfall simulator, two repetitions of rainfall simulation were carried out for each H-T combination. Before each simulation, the Falcon® 50 ml PP conical tubes has been weighed, representing the tare, and then the rainfall intensity of each nozzle has been obtained by referring the net weight to the unit time and area (equal to 0.001276 m^2 obtained by the ratio between the area of the simulator plate and the number of nozzles). To ensure that the collector system could collect the total amount of simulated rainfall, a control rainfall simulation was performed by measuring, for each H-T combination, the total volume of rainfall discharged into a tank. This procedure yielded a total of 33 rainfall simulations.

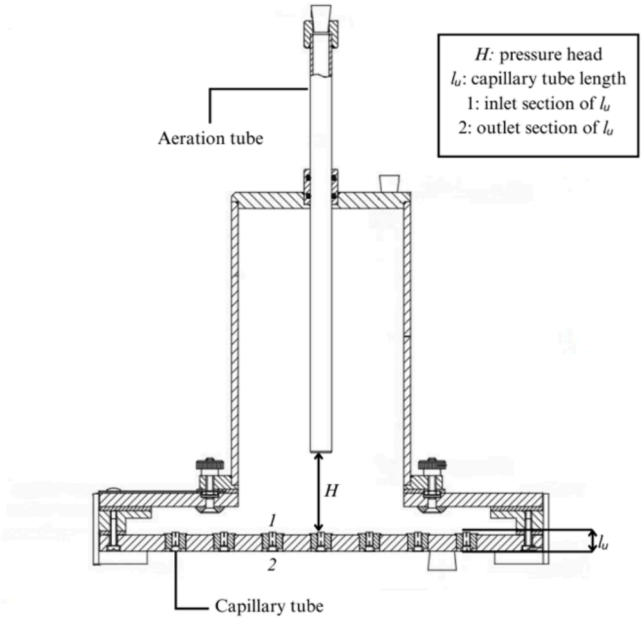

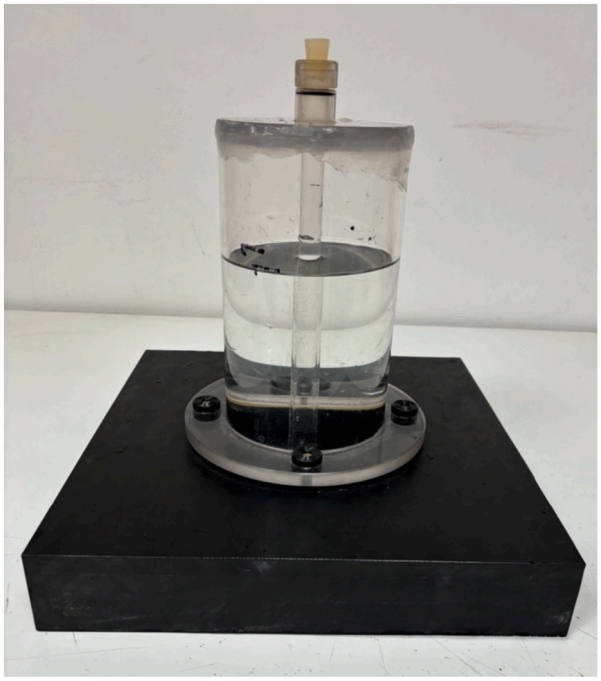

Fig. 2. Vertical cross section and view of the sprinkler head.

2.3. Test procedure to determine rainfall characteristics and calculate rainfall kinetic power and momentum

To characterize the rainfall simulator from a rainfall kinetic energy point of view, a standardized test procedure was performed using different values of water temperatures, T, and pressure heads, H. For each H-T pair, which was repeated three times, the water volume corresponding to 100 water drops flowing out by the selected capillary tube was collected and weighed, and the sampling time was recorded.

The knowledge of the weight of the water volume, m (kg), referred to the considered number of the drops, n_D, allows to determine the mean mass of a single water drop, m_{SD} (kg), as follows:

$$m_{SD} = \frac{m}{n_D} \tag{4}$$

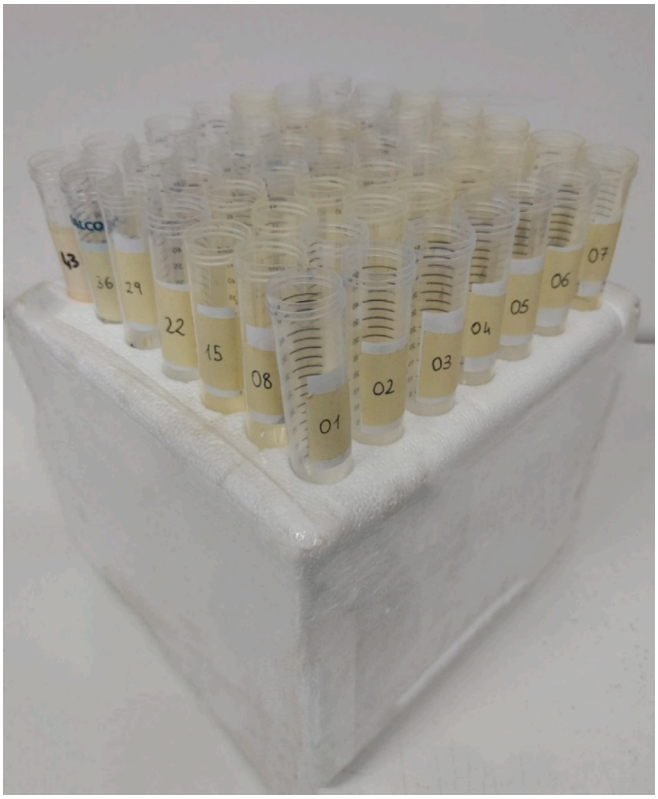

Fig. 3. View of the **r**ainfall intensity collector system.

Considering H equal to 1.9 cm, 4.9 cm, and 6.9 cm and water temperature ranging from 16 °C to 26.1 °C, the fall velocity of a droplet, v (m s^{-1}) was determined by a photographic method. For each H value, four falling height intervals (h = 0.33–0.42 m; h = 0.52–0.61 m; h = 0.85–0.96 m; h = 1.21–1.30 m) were used. Measuring the displacement of a single raindrop between two following frames, looking at its upper tip, and knowing the frame rate, the raindrop fall velocity, v (m s^{-1}), was calculated. A maximum value of H equal to 6.9 cm is fixed in this investigation because, beyond this value, more raindrops have been detected in a given frame and this circumstance made difficult to identify the path of the considered falling raindrop.

For each test condition, the knowledge of mass, m, and fall velocity of the droplets, v, which was assumed the same for all drops, yielded to calculate both the kinetic power, P_n (J m^{-2} s^{-1}), and momentum, M (N m^{-2}), per unit time and area:

$$P_n = \frac{\frac{1}{2}mv^2}{\sigma t} \tag{5}$$

$$M = \frac{mv}{\sigma t} \tag{6}$$

in which t (s) is the sampling time and σ is the area assigned to the considered capillary tube that is equal to 0.001276 m^2.

The reliability of the photographic method to estimate the raindrop fall velocity was checked through a comparison between v values and the maximum velocity, v_{max} (m s^{-1}), that a drop, starting from a standstill, could acquire by falling free in a vacuum, from a height h (m), in the absence of friction due to air resistance:

$$v_{max} = \sqrt{2gh} \tag{7}$$

According to this relation, the falling height is the only variable that influences v_{max}.

3. Results

To evaluate the uniform rainfall intensity distribution of the Kamphorst simulator the procedure described in the Section 2.2 has been used. For different test conditions T (24–27 °C) and H (1.9–11.9 cm) the values of the simulated rainfall intensity of each capillary tube, I_i (mm h^{-1}), have been measured and the mean value of the simulator rainfall intensity, I_S (mm h^{-1}) has been calculated.

Fig. 4 shows, as an example, the spatial rainfall intensity distribution for H-T values equal to 1.9 cm and 26.1 °C, 5.9 cm and 26.6 °C, 8.9 cm and 26.6 °C, and 11.9 cm and 25.7 °C. To standardize its schematic representation for different test conditions, the ratio γ_i, between I_i (mm h^{-1}), and I_S (mm h^{-1}), was calculated. A γ_i value equal to 1 represents a condition of correct functioning of the capillary tube.

In this analysis, 10 ranges of γ values have been considered, each of which was attributed a different color (Fig. 4). The experimental data stated that γ_i assumes values between 0.64 and 1.08 because some nozzle gave an $I_i > I_S$ ($\gamma_i > 1$) or $I_i < I_S$ ($\gamma_i < 1$). However, the analysis confirmed the correct functioning of the simulator since, on average, 89.80 % of the nozzles gave an I_i equal to I_S (Table 1). For each considered H, Table 1 shows the values of the Christiansen Uniformity coefficient CU (%), highlighting a mean value of CU equal to 97.24 %.

These results supported the hypothesis that the experimental runs finalized to the energetic characterization of the Kamphorst simulator can be carried out considering the functioning of one capillary tube.

To study the influence of the water temperature on the raindrop mass, m_{SD} (mg), Fig. 5 shows the relationship between, m_{SD} values calculated by Eq. (4), and the pressure head, H (m), for different water temperatures, T (°C), measured at the outlet of the considered capillary tube. For a fixed T, the measurements highlighted that the m_{SD} value

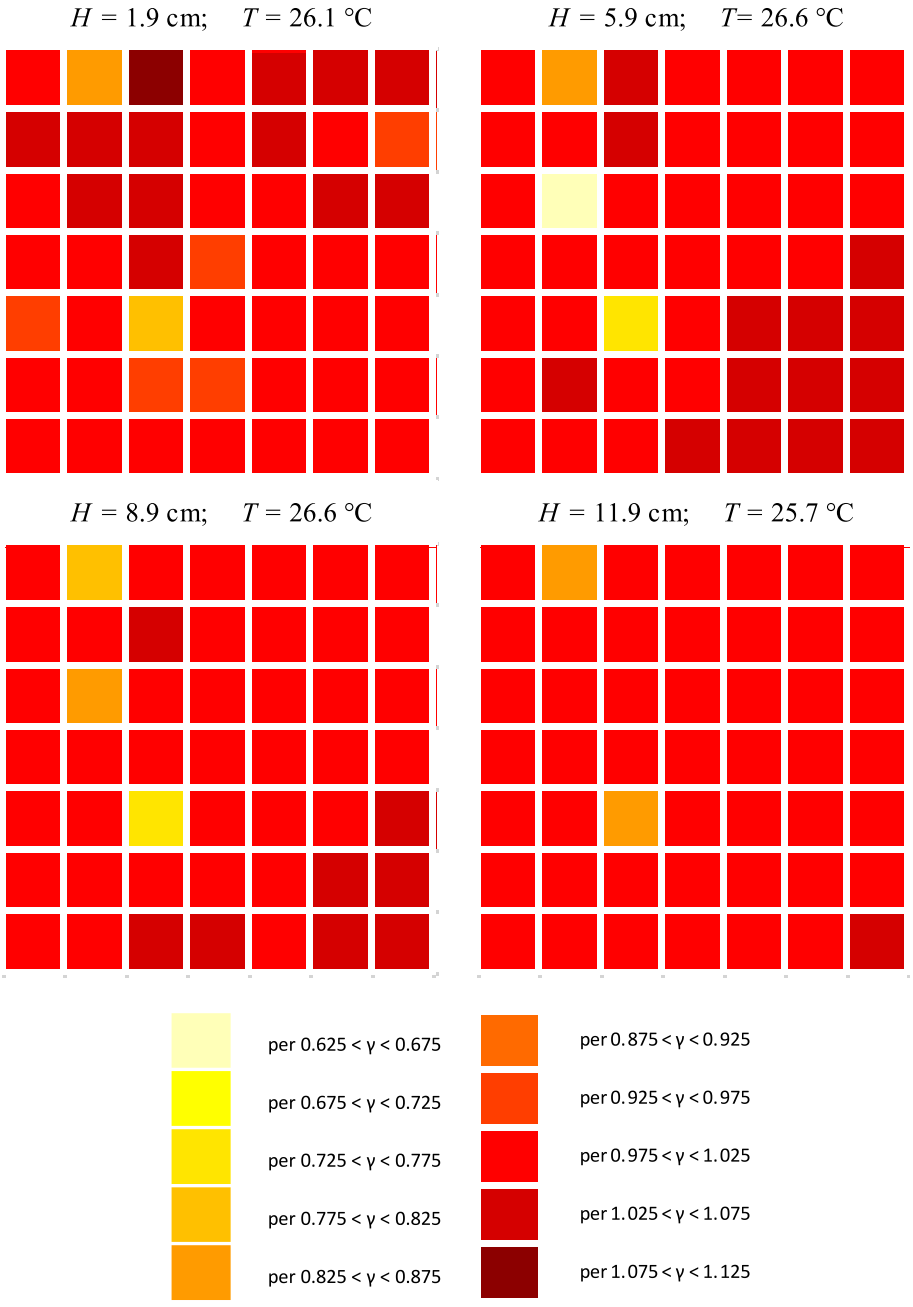

Fig. 4. Plot of γ_i values representing the rainfall intensity uniformity distribution.

Table 1
Rainfall intensity *CU* for a fixed *H* value.

H [cm]	*CU* [%]	$0.95 \leq \gamma < 1.05$
1.9	96 %	78.6 %
2.9	97 %	84.7 %
3.9	97 %	82.7 %
4.9	97 %	92.9 %
5.9	97 %	86.7 %
6.9	96 %	88.8 %
7.9	98 %	95.9 %
8.9	97 %	93.9 %
9.9	97 %	91.8 %
10.9	99 %	95.9 %
11.9	99 %	95.9 %
Mean value [%]	97.24 %	89.80 %

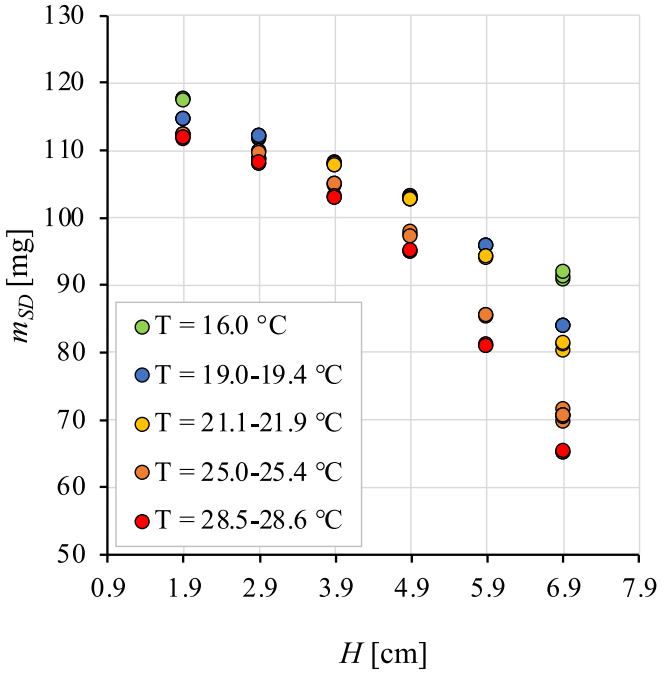

Fig. 5. Relationship between m_{SD} and H values for different water temperatures.

decreases as H increases. Moreover, for a fixed H value, the growth of the water temperature determines a decrease in the m_{SD} value.

For different H and T values, the relationship between m_{SD} and I_S is plotted in Fig. 6. The measures show that I_S ranges from 187.8 to 633.7 mm h^{-1} and m_{SD} varies from 65.1 to 117.7 mg. The m_{SD} values present a decreasing trend with I_S and this trend is independent of the considered pressure head (Fig. 6**a**) and water temperature (Fig. 6**b**) values. This figure also shows that the highest values of H and of T produced the highest I_S and the smallest m_{SD} values. Moreover, the experimental pairs (I_S, m_{SD}) suggest a threshold value of I_S equal to 500 mm h^{-1}, corresponding to H>4.9 cm for the present investigation, over which the rate of the raindrop mass reduction is much higher than that corresponding to $H \leq 4.9$ cm (Fig. 7).

As described in Section 2.3, for each considered pressure head and water temperature, raindrop fall velocity values, v (m s^{-1}), were measured at different falling heights, h (m), by the photographic method. The reliability of the photographic method was checked through a comparison between the values of measured v and the theoretical velocity, v_{max} (m s^{-1}), obtained by Eq. (7) (Fig. 8). The experimental pairs (v_{max}, v) are below the 1:1 line, suggesting the reliability of the raindrop velocity measurements obtained by the photographic method. Furthermore, for this simulator and the investigated h values,

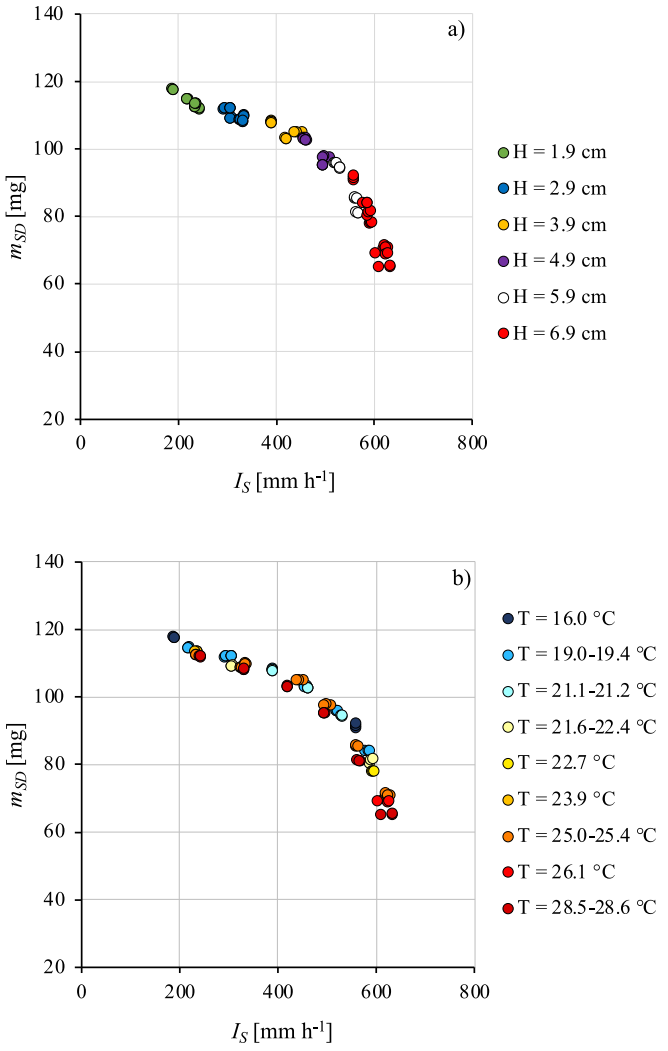

Fig. 6. Relationship between m_{SD} and I_S for different H (a) and T (b) values.

these results suggested that the fall velocity v_f (m s^{-1}) can be calculated as:

$$v_f = \omega\sqrt{2gh} \tag{8}$$

in which ω is a dimensionless constant that has been estimated by fitting Eq. (8) to empirical fall velocity measurements carried with photographic technique. For each considered H value, Fig. 9 shows the comparison between the values of measured v and v_f calculated by Eq. (8). The analysis confirms that the photographic method considered in the present investigation employs raindrop fall velocity values that are, on average, 5 % lower than those obtained by Eq. (7). Moreover, the low variability of ω, that ranges from 0.9490 to 0.9576, suggested to assume a constant value of 0.9525, equal to the mean value of ω values.

Therefore, substituting v with v_f, in Eqs. (5) and (6), they became:

$$P_n = \frac{gm\omega^2 h}{\sigma t} \tag{9}$$

$$M = (2g)^{0.5}\frac{m\omega h^{0.5}}{\sigma t} \tag{10}$$

Moreover, since that:

$$\frac{m}{\sigma t} = I_S\rho \tag{11}$$

Eqs. (9) and (10) can be rewritten as:

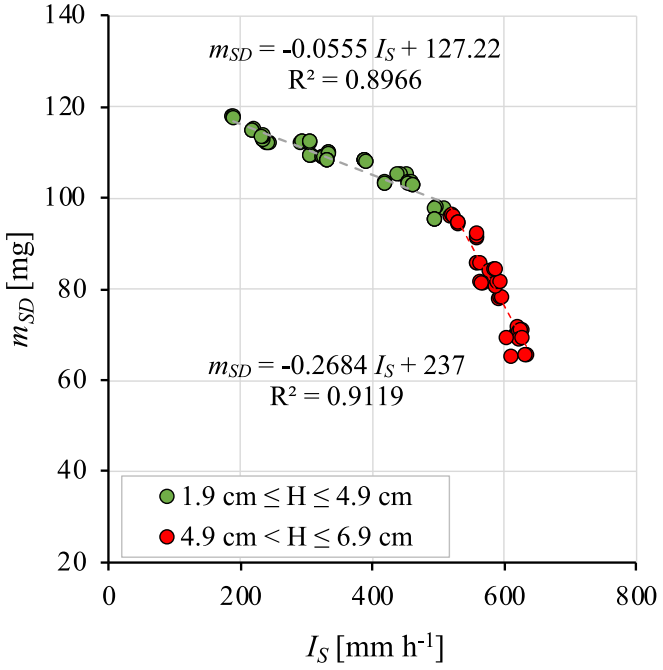

Fig. 7. Relationship between m_{SD} and I_S for two different range of H.

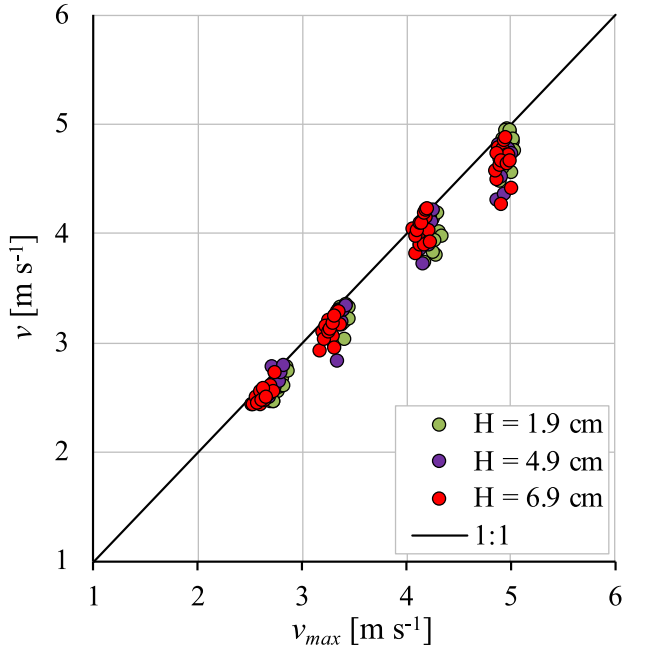

Fig. 8. Comparison between the values of fall velocity calculated by Eq. (7), v_{max}, and those measured, v, for different H values.

$$P_n = g\omega^2\rho h I_S \tag{12}$$

$$M = (2g)^{0.5}\omega\rho h^{0.5} I_S \tag{13}$$

These relationships allow to characterize from an energetic point of view the rainfall simulator by the only knowledge of h and I_S.

Fig. 10 shows the comparison between the rainfall kinetic power and momentum obtained by Eqs. (5) and (6) and those estimated by Eqs. (12) and (13) respectively, in which ω is equal to 0.9525. As the data pairs are near the perfect agreement line, this result is a confirmation of the reliability of Eqs. (12) and (13) to estimate the kinetic power and

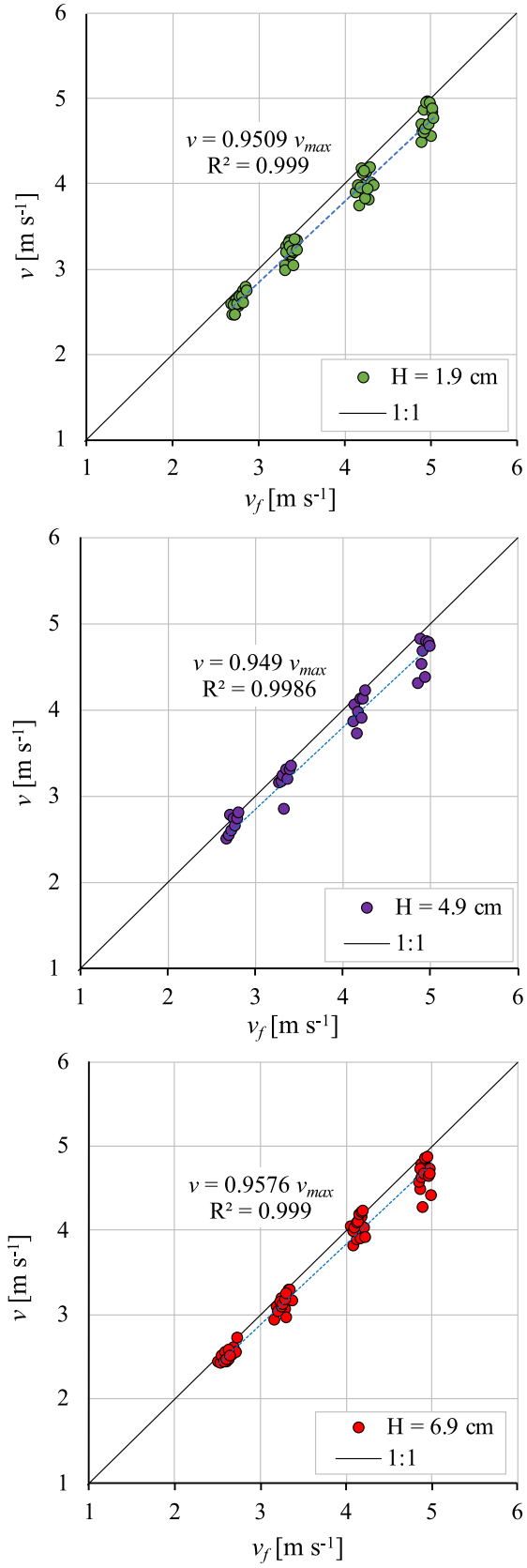

Fig. 9. Relationship between the measured values of v and those estimated by Eq. (8) for different H values.

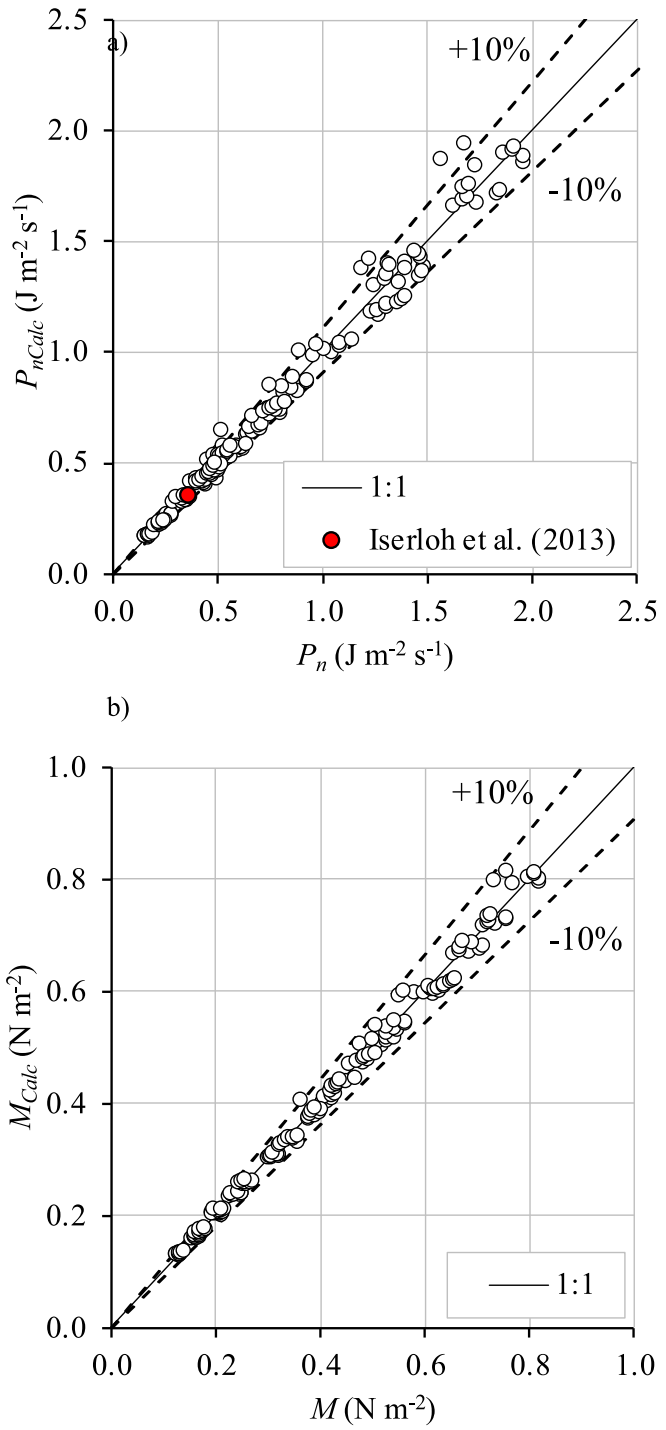

Fig. 10. Comparison between the measured values of P_n (a) and M (b) and those estimated by Eq. (12) and Eq. (13), respectively.

momentum, respectively. Concerning the kinetic power, in Fig. 10**a** the point corresponding to the P_n value measured by Iserloh et al. (2013) and that calculated by Eq. (12), using the operating condition reported by Iserloh et al. (2013) (I_S=360 mm h^{-1} and h = 0.40 m) is also plotted. The point is overlapped to those of the present investigation, confirming the reliability of the proposed method to characterize energetically the Kamphorst simulator.

The errors E (%) in P_n and M estimates (Fig. 11) range from −12.76 % to 25.68 % for P_n and from −6.69 % to 11.99 % for M. Moreover, the 88.75 % for P_n and 99.38 % for M of measurements are affected by a mean absolute error, MAE, less than 10 % (Table 2).

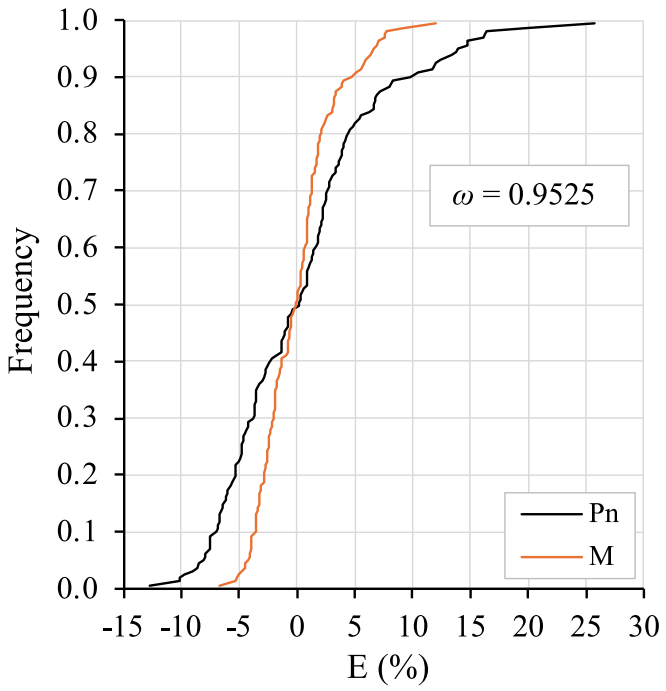

Fig. 11. Empirical frequency distribution of errors E in P_n and M estimates obtained by Eq. (12) and Eq. (13), respectively.

Table 2
Reliability of Eqs. (12) and (13) to P_n and M estimates for the Kamphorst simulator.

	P_n	M
Mean Relative Error (MRE)	0.37 %	0.03 %
Mean Absolute Error (MAE)	5.12 %	2.54 %
Percentage of measurement with MAE≤10 %	88.75 %	99.38 %

Finally, the I_s measurements have been used to test the reliability of Eq. (3) to estimate rainfall intensity with α_1 = 1.25. As expected, in accordance with Agosta et al. (2022), the closeness of the points to the line of perfect agreement represents a confirmation of the reliability of Eq. (3) to estimate rainfall intensity per unit area and time (Fig. 12). The I_s measurements suggested that the use of Eq. (3) produces an underestimation of the I_s values equal to −0.30 % and the 90.91 % of the measurements are affected by errors less than or equal to ± 5 %. Therefore, the knowledge of both the operating conditions (T and H) and the rainfall simulator geometric characteristics (d and l_{ii}) allow to have a good estimation of the simulated rainfall intensity.

4. Discussion

In this investigation, at first, the rainfall intensity uniformity distribution of the Kamphorst simulator for different test conditions (T; H) was positively tested, as shown in Fig. 4. The use of different colors attributed to γ values for representing the functioning of each capillary tube, allowed to verify that only few capillary tubes didn't give a rainfall intensity equal to I_S. Probably, the incorrect functioning can be due to partial obstructions of the capillary tube hole. However, a mean value of CU equal to 97.24 % has been obtained, considering the variations in T and H values. In agreement with Iserloh et al. (2013), this result allows to conclude that a mean CU value (%), greater than 80 % guarantees the correct functioning and reproducibility of rainfall intensity simulation experiments.

For different H and T values, the raindrop mass showed a decreasing trend with H, independently of the water temperature, due to the

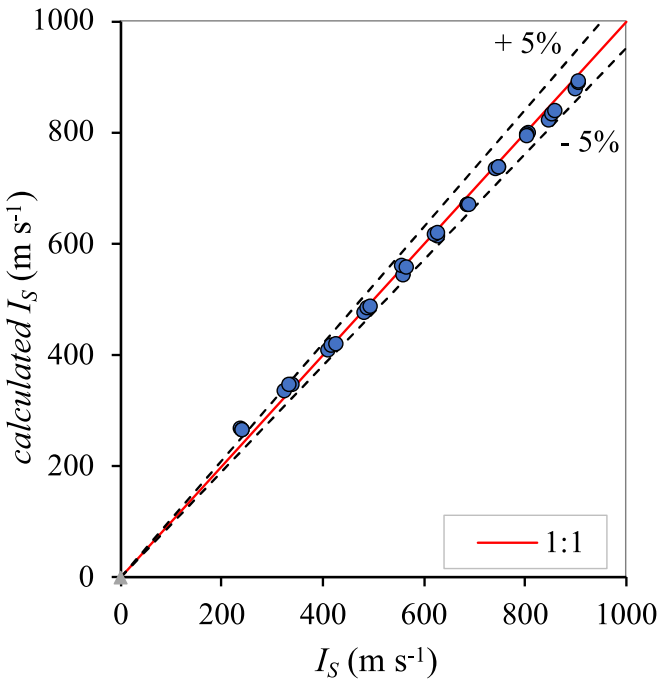

Fig. 12. Comparison between the measured I_S values and those calculated by Eq. (3).

variation of the simulated rainfall intensity. In fact, the growth of the water temperature determined a reduction of m_{SD} due to a decrease of water viscosity and thus an increase of outflow velocity occurred. Furthermore, the outflow velocity is also influenced by the increase of H. In other words, since H and T determine I_s, as a consequence the latter is the only variable that influences the m_{SD} formation of the simulated rainfall, because it summarizes the influence of H and T on m_{SD}. In particular, the increase of I_s, due to a growth of H and/or T, determines a decrease in m_{SD} because, in a given sampling time, the rate of the raindrop formation at the outlet of the nozzle increases, and this circumstance yields to have many drops characterized by low m_{SD} values.

For each considered pressure head and water temperature, fall velocity measurements, v (m/s), were also carried out for h lower than 1.3 m, that was the maximum explorable value for the experimental setup considered in this investigation. The measurements suggested that the fall velocity is only dependent on h, presenting an increasing trend with h and this result is independent on the considered pressure head. Moreover, the closeness of the experimental points of the pairs (h, v) to the curve of Eq. (7), supported the reliability of the velocity measurements by the photographic method. Moreover, these results suggested that, for $h < 1.3$ m, the behavior of the simulated raindrop is similar to that of a drop that falls free in a vacuum. The analysis also highlighted that Eq. (7) overestimates the raindrop fall velocities with respect to the measured values and this result could be due to the effects of the air resistance during the drop falling motion. In other words, for h lower than 1.3 m, a reliable estimate of the simulated raindrop fall velocity can be obtained by applying Eq. (8) for the known falling height.

The developed analysis suggested that, for the simulated rainfall, P_n and M are function of h and $\sqrt{h}$, respectively, and I_s, since the raindrop mass only depends on I_s and the raindrop fall velocity, for $h < 1.3$ m, is only a function of 0.9525 $\sqrt{h}$. Therefore, for the Kamphorst's simulator, two relationships to calculate P_n (Eq. (12) and M (Eq. (13) have been proposed. The comparison between the measured values of P_n and M and those estimated by Eq. (12) and Eq. (13), respectively, (Fig. 10) suggested that for $h < 1.3$ m the knowledge of both the simulated rainfall intensity and the raindrop falling height yielded to have accurate estimations of the kinetic power and momentum of the rainfall produced by the Kamphorst's simulator. Moreover, the best performance of M estimates is due to the circumstance that M depends on $\sqrt{h}$, and the effect of the estimate error of fall velocity is lower than P_n one, that depends on h. The reliability of Eq. (12) has been also positively tested using Iserloh et al. (2013) measurements of P_n, h and Is carried out using the same rainfall simulator. In fact, the use of Eq. (12), that requires the knowledge of the simulated rainfall intensity and of the raindrop falling height, allowed to have the same value measured by Iserloh et al. (2013).

For this simulator and low falling heights, the setting of pressure head, H, water temperature, T, and falling height, h, is sufficient for having a complete energetic characterization of the simulated rainfall.

The relationship theoretically deduced by Agosta et al. (2022) to estimate the rainfall intensity of the Kamphorst simulator, Eq. (3), was also tested. The measurements of I_s carried out in different test conditions (H and T) allowed us to positively verify the reliability of Eq. (3). Therefore, the knowledge of both the operating conditions (T and H) and the rainfall simulator geometric characteristics (d and l_u) allowed to have a good estimation of the simulated rainfall intensity.

From an operative point of view, the analysis developed in this investigation yielded to have operative information about the characterization of the Kamphorst simulator. In fact, the use of Eq. (3) allowed to have accurate estimates of the rainfall intensity, by only measuring the pressure head, water temperature, and knowing the values of the geometric characteristics of the capillary tube, i.e. diameter and length. Moreover, with reference to this simulator and for low falling height ($h < 1.3$ m), the measurement of I_s and h is sufficient to obtain a reliable estimate of P_n and M. In other words, the knowledge of the geometric characteristics of the capillary tube, the pressure head, water temperature and falling height values are fundamental for having a complete characterization of the rainfall simulator because these variables allow to determine I_s, P_n, and M.

5. Conclusion

Rainfall simulators, providing controlled conditions for investigating hydrological and erosive processes, are valuable tools for the scientific research of soil erosion processes. To date, one of the most widely employed simulators for its ease of use and its small size is that developed by Eijkelkamp and described by Kamphorst.

It is well known that the main and critical properties of a simulated rainfall are the determination of its spatial distribution on the plot area, the drop size distribution (DSD), the fall velocity of the drops, and consequently the kinetic energy and momentum discharged to the soil. Nevertheless, until now, no author has characterized the Kamphorst simulator, for different pressure heads, water temperature, and falling height values.

Therefore, the aim of this investigation was to give operating instructions, for several working conditions, on the functionality of the Kamphorst simulator in terms of simulated rainfall uniformity distribution and kinetic energy and momentum discharged to the soil.

This analysis showed that, for several test conditions (temperature and pressure heads), the Kamphorst rainfall simulator has very good performances in terms of intensity uniformity distribution. This result allowed us to consider the use of a single nozzle for the energetic characterization, performed by coupling the weighing technique for the determination of the raindrop mass and the photographic technique for the detection of its fall velocity.

The developed analysis also revealed that rainfall intensity, depending on pressure head and water temperature, is the only variable that affects the mean mass of a single drop. For each test condition the raindrop mass presented a decreasing trend with rainfall intensity, since an increase of outflow velocity occurred. Moreover, the analysis suggested that for this simulator and small falling height ($h < 1.3$ m),

droplets come out with fall velocities comparable to that of a body falling free in a vacuum. From the operational point of view, this is a huge advantage, since it allows to estimate fall velocity only knowing the falling height, without considering more complex techniques for obtaining raindrop v values.

New empirical relationships for estimating rainfall kinetic power and momentum by the knowledge of both simulated rainfall intensity and falling height have been proposed and verified considering the P_n and M values obtained by fall drop velocity and mass measurements.

Finally, from the operative point of view, this investigation yielded to conclude that to characterize the Kamphorst's simulator it is enough to know the geometric characteristics of the nozzle, pressure head, water temperature, and falling height values.

An objective of future investigations could be to study a modification of the Kamphorst simulator by choosing materials or geometries (lengths, internal diameter) of the capillary tubes (nozzles, needles) different from the manufacturing ones.

CRediT authorship contribution statement

F.G. Carollo: Writing – review & editing, Visualization, Validation, Supervision, Methodology, Formal analysis, Data curation, Conceptualization. **R. Caruso:** Writing – review & editing, Writing – original draft, Methodology, Formal analysis, Data curation. **V. Ferro:** Writing – review & editing, Writing – original draft, Visualization, Validation, Supervision, Methodology, Formal analysis, Data curation, Conceptualization. **M.A. Serio:** Writing – review & editing, Writing – original draft, Visualization, Methodology, Formal analysis, Data curation, Conceptualization.

Declaration of competing interest

The authors declare that they have no known competing financial interests or personal relationships that could have appeared to influence the work reported in this paper.

Data availability

Data will be made available on request.

Acknowledgements

All authors set up the research, analyzed and interpreted the results and contributed to write the paper.

This research is founding by "SiciliAn MicronanOTecH Research And Innovation CEnter "SAMOTHRACE" (MUR, PNRR-M4C2, ECS_00000022), spoke 3 - Università degli Studi di Palermo "S2-COMMs - Micro and Nanotechnologies for Smart & Sustainable Communities".

References

Abudi, I., Carmi, G., Berliner, P., 2012. Rainfall simulator for field runoff studies. J. Hydrol. 454, 76–81. https://doi.org/10.1016/j.jhydrol.2012.05.056.

Adams, J.E., Kirkham, D., Nielsen, D.R., 1957. A portable rainfall-simulator infiltrometer and physical measurements of soil in place. Soil Sci. Soc. Am J 21 (5), 473–477. https://doi.org/10.2136/sssaj1957.03615995002100050004x.

Agosta, M., Bagarello, V., Caltabellotta, G., Carollo, F.G., Vaccaro, G., Pampalone, V., 2022. Theoretical prediction of rainfall intensity for a small rainfall simulator. In 2022 IEEE Workshop on Metrology for Agriculture and Forestry (MetroAgriFor) (pp. 329-333). IEEE. doi: 10.1109/MetroAgriFor55389.2022.9965068.

Alves Sobrinho, T., Gómez-Macpherson, H., Gómez, J.A., 2008. A portable integrated rainfall and overland flow simulator. Soil Use Manag. 24 (2), 163–170. https://doi.org/10.1111/j.1475-2743.2008.00150.x.

Bagarello, V., Baiamonte, G., Ferro, V., Giordano, G., 1996. Contributo alla valutazione dei fattori elementari dell'erosione negli studi a scala di bacino. Quad. Idron. Mont. 15, 47–82.

Bagarello, V., Ferro, V., 2004. Plot-scale measurement of soil erosion at the experimental area of Sparacia (southern Italy). Hydrol. Process. 18 (1), 141–157. https://doi.org/10.1002/hyp.1318.

Bahddou, S., Otten, W., Whalley, W.R., Shin, H.C., El Gharous, M., Rickson, R.J., 2023. Changes in soil surface properties under simulated rainfall and the effect of surface roughness on runoff, infiltration and soil loss. Geoderma 431, 116341. https://doi.org/10.1016/j.geoderma.2023.116341.

Battany, M.C., Grismer, M.E., 2000. Development of a portable field rainfall simulator for use in hillside vineyard runoff and erosion studies. Hydrol. Process. 14 (6), 1119–1129. https://doi.org/10.1002/(SICI)1099-1085(20000430)14:6<1119::AID-HYP8>3.0.CO;2-O.

Birt, L.N., Persyn, R.A., Smith, P.K., 2007. Evaluation of an indoor nozzle-type rainfall simulator. Appl. Eng. Agric. 23 (3), 283–287. https://doi.org/10.13031/2013.22689.

Blanquies, J., Scharff, M., Hallock, B., 2003. The design and construction of a rainfall simulator. International Erosion Control Association (IECA), 34th Annual Conference and Expo., Las Vegas, Nevada, February 24-28, 2003.

Boulal, H., Gómez-Macpherson, H., Gómez, J.A., Mateos, L., 2011. Effect of soil management and traffic on soil erosion in irrigated annual crops. Soil Tillage Res. 115, 62–70. https://doi.org/10.1016/j.still.2011.07.003.

Brandt, C.J., 1989. The size distribution of throughfall drops under vegetation canopies. Catena 16 (4–5), 507–524. https://doi.org/10.1016/0341-8162(89)90032-5.

Bryan, R.B., 1974. A simulated rainfall test for the prediction of soil erodibility. Z. Geomorph. Suppl. Bard. 21, 138–150.

Calvo, A., Gisbert, J.M., Palau, E., Romero, M., 1988. Un simulador de lluvia portátil de fácil construcción. In: Sala, M., Gallart, F. (Eds.), Métodos y Técnicas Para La Medición En El Campo De Procesos Geomorfo-Lógicos. Soc Esp. Geomorf, Zaragoza, pp. 6–15.

Carollo, F.G., Ferro, V., Serio, M.A., 2017. Reliability of rainfall kinetic power–intensity relationships. Hydrol. Process. 31 (6), 1293–1300. https://doi.org/10.1002/hyp.11099.

Carollo, F.G., Ferro, V., Serio, M.A., 2018a. Predicting rainfall erosivity by momentum and kinetic energy in Mediterranean environment. J. Hydrol. 560, 173–183. https://doi.org/10.1016/j.jhydrol.2018.03.026.

Carollo, F.G., Serio, M.A., Ferro, V., Cerdà, A., 2018b. Characterizing rainfall erosivity by kinetic power-median volume diameter relationship. Catena 165, 12–21. https://doi.org/10.1016/j.catena.2018.01.024.

Cerdà, A., Ibáñez, S., Calvo, A., 1997. Design and operation of a small and portable rainfall simulator for rugged terrain. Soil Technol. 11 (2), 163–170. https://doi.org/10.1016/S0933-3630(96)00135-3.

Christiansen, J.E., 1942. Irrigation by Sprinkling, Vol. 4. University of California, Berkeley.

Clarke, M.A., Walsh, R.P., 2007. A portable rainfall simulator for field assessment of splash and slopewash in remote locations. Earth Surf. Process. Landf: J. Br. Geomorphol. Res. Gr. 32 (13), 2052–2069. https://doi.org/10.1002/esp.1526.

Covert, A., Jordan, P., 2009. A portable rainfall simulator: techniques for understanding the effects of rainfall on soil erodibility. Streamline Watershed Manag. Bull. 13 (1), 5–9.

De Ploey, J., 1981. Crusting and time-dependent rainwash mechanisms on loamy soil. In: Morgan, R.P.C. (Ed.), Soil Conservation Problems and Prospects. Wiley, pp. 139–154.

Eijkelkamp, 2022. Rainfall simulator - Operating instructions, M-0906E. https://www.royaleijkelkamp.com/media/1awdmlno/m-0906e-rainfall-simulator.pdf.

Etheridge, J.A., 2023. Construction and Calibration of Large-Scale Rainfall Simulators (Doctoral dissertation, Auburn University).

Farres, P.J., 1987. The dynamics of rainsplash erosion and the role of soil aggregate stability. Catena 14 (1–3), 119–130. https://doi.org/10.1016/S0341-8162(87)80009-7.

Gunn, R., Kinzer, G.D., 1949. The terminal velocity of fall for water droplets in stagnant air. J. Atmos. Sci. 6 (4), 243–248. https://doi.org/10.1175/1520-0469(1949)006<0243:TTVOFF>2.0.CO;2.

Hassel, J., Richter, G., 1988. Die Niederschlagsstruktur des Trierer Regensimulators. Mitt. Ditsch. Bodenkd. Ges. 56, 93–96.

Hudson, N.W., 1963. Raindrop characteristics in south central United States. Rhod. J. Agric. Res. 1, 6–11.

Hudson, N.W., 1965. The influence of rainfall on the mechanics of soil erosion: with particular reference to Southern Rhodesia (Master's thesis, University of Cape Town).

Humphry, J.B., Daniel, T.C., Edwards, D.R., Sharpley, A.N., 2002. A portable rainfall simulator for plot–scale runoff studies. Appl. Eng. Agric. 18 (2), 199. https://doi.org/10.13031/2013.7789.

Imeson, A.C., 1977. A simple field-portable rainfall simulator for difficult terrain. Earth Surf. Process. 2 (4), 431–436. https://doi.org/10.1002/esp.3290020414.

Iserloh, T., Ries, J.B., Arnáez, J., Boix-Fayos, C., Butzen, V., Cerdà, A., Echeverría, M.T., Fernández-Gálvez, J., Fister, W., Geißler, C., Gómez, J.A., Gómez-Macpherson, H., Kuhn, N.J., Lázaro, R., León, F.J., Martínez-Mena, M., Martínez-Murillo, J.F., Marzen, M., Mingorance, M.D., Ortigosa, L., Peters, P., Regüés, D., Ruiz-Sinoga, J.D., Scholten, T., Seeger, M., Solé-Benet, A., Wengel, R., Wirtz, S., 2013. European small portable rainfall simulators: A comparison of rainfall characteristics. Catena 110, 100–112. https://doi.org/10.1016/j.catena.2013.05.013.

Joss, J., Waldvogel, A., 1967. Ein spektrograph für niederschlagstropfen mit automatischer auswertung. Pure Appl. Geophys. 68, 240–246. https://doi.org/10.1007/BF00874898.

Kalehhouei, M., Sadeghi, S.H., Darvishan, A.K., 2023. Changes in raindrop properties due to wind blowing using image processing. Catena 221, 106789. https://doi.org/10.1016/j.catena.2022.106789.

Kamphorst, A., 1987. A small rainfall simulator for the determination of soil erodibility. Neth. J. Agric. Sci. 35 (3), 407–415. https://doi.org/10.18174/njas.v35i3.16735.

Kavian, A., Mohammadi, M., Cerdà, A., Fallah, M., Abdollahi, Z., 2018. Simulated raindrop's characteristic measurements. A new approach of image processing tested under laboratory rainfall simulation. Catena 167, 190–197. https://doi.org/10.1016/j.catena.2018.04.034.

Lascano, R.J., Vorheis, J.T., Baumhardt, R.L., Salisbury, D.R., 1997. Computer-controlled variable intensity rain simulator. Soil Sci. Soc. Am. J. 61 (4), 1182–1189. https://doi.org/10.2136/sssaj1997.03615995006100040025x.

Lascelles, B., Favis-Mortlock, D.T., Parsons, A.J., Guerra, A.J.T., 2000. Spatial and temporal variation in two rainfall simulators: implications for spatially explicit rainfall simulation experiments. Earth Surf. Process. Landf. 25 (7), 709–721. https://doi.org/10.1002/1096-9837(200007)25:7<709::AID-ESP126>3.0.CO;2-K.

Laws, J.O., Parsons, D.A., 1943. The relation of raindrop-size to intensity. Eos, Trans. Am. Geophys. Un. 24 (2), 452–460. https://doi.org/10.1029/TR024i002p00452.

Loch, R.J., Robotham, B.G., Zeller, L., Masterman, N., Orange, D.N., Bridge, B.J., Sheridan, G.J., Bourke, J.J., 2001. A multi-purpose rainfall simulator for field infiltration and erosion studies. Soil Res. 39 (3), 599–610. https://doi.org/10.1071/SR00039.

Luk, S.H., 1985. Effect of antecedent soil moisture content on rainwash erosion. Catena 12 (2–3), 129–139. https://doi.org/10.1016/0341-8162(85)90005-0.

Martínez-Mena, M., Abadía, R., Castillo, V., Albaladejo, J., 2001. Diseño experimental mediante lluvia simulada para el estudio de los cambios en la erosión del suelo durante la tormenta. Cuatern. Geomorfol 15 (1–2), 31–43.

Nadal-Romero, E., Regüés, D., 2009. Detachment and infiltration variations as consequence of regolith development in a Pyrenean badland system. Earth Surf. Process. Landf. 34 (6), 824–838. https://doi.org/10.1002/esp.1772.

Neal, J.H., 1938. The effect of the degree of slope and rainfall characteristics on runoff and soil erosion. University of Missouri, College of Agriculture, Agricultural Experiment Station.

Norton, L.D., 1987. Micromorphological study of surface seals developed under simulated rainfall. Geoderma 40 (1–2), 127–140. https://doi.org/10.1016/0016-7061(87)90018-8.

Poesen, J., Ingelmo-Sanchez, F., Mucher, H., 1990. The hydrological response of soil surfaces to rainfall as affected by cover and position of rock fragments in the top layer. Earth Surf. Process. Landf. 15 (7), 653–671. https://doi.org/10.1002/esp.3290150707.

Regmi, T.P., Thompson, A.L., 2000. Rainfall simulator for laboratory studies. Appl. Eng. Agric. 16 (6), 641–647. https://doi.org/10.13031/2013.5380.

Regüés, D., Gallart, F., 2004. Seasonal patterns of runoff and erosion responses to simulated rainfall in a badland area in Mediterranean mountain conditions (Vallcebre, southeastern Pyrenees). Earth Surf. Process. Landf. 29 (6), 755–767. https://doi.org/10.1002/esp.1067.

Ries, J.B., Langer, M., 2001. Runoff generation on abandoned fields in the Central Ebro Basin. Results from rainfall simulation experiments. Cuad. Investig. Geográf.: Geogr. Res. Lett. 27, 61–78.

Ries, J.B., Langer, M., Rehberg, C., 2000. Experimental investigations on water and wind erosion on abandoned fields and arable land in the central Ebro Basin. Aragón/spain. z. Geomorphol. 121, 91–108.

Ries, J.B., Seeger, M., Iserloh, T., Wistorf, S., Fister, W., 2009. Calibration of simulated rainfall characteristics for the study of soil erosion on agricultural land. Soil Tillage Res. 106 (1), 109–116. https://doi.org/10.1016/j.still.2009.07.005.

Ries, J.B., Iserloh, T., Seeger, M., Gabriels, D., 2013. Rainfall simulations-constraints, needs and challenges for a future use in soil erosion research. Supplementary Issues Zeitschrift für Geomorphologie 57 (1), 1–10. https://doi.org/10.1127/0372-8854/2013/S-00130.

Roth, C.H., Meyer, B., Frede, H.G., 1985. A portable rainfall simulator for studying factors affecting runoff, infiltration and soil loss. Catena 12 (1), 79–85. https://doi.org/10.1016/S0341-8162(85)80006-0.

Sadeghi, S.H., Abdollahi, Z., Darvishan, A.K., 2013. Experimental comparison of some techniques for estimating natural raindrop size distribution on the south coast of the Caspian Sea. Iran. Hydrol. Sci. J. 58 (6), 1374–1382. https://doi.org/10.1080/02626667.2013.814917.

Salles, C., Poesen, J., 1999. Performance of an optical spectro pluviometer in measuring basic rain erosivity characteristics. J. Hydrol. 218 (3–4), 142–156. https://doi.org/10.1016/S0022-1694(99)00031-1.

Salles, C., Poesen, J., Borselli, L., 1999. Measurement of simulated drop size distribution with an optical spectro pluviometer: sample size considerations. Earth Surf. Process. Landf. 24 (6), 545–556. https://doi.org/10.1002/(SICI)1096-9837(199906)24:6<545::AID-ESP3>3.0.CO;2-D.

Seeger, M., 2007. Uncertainty of factors determining runoff and erosion processes as quantified by rainfall simulations. Catena 71 (1), 56–67. https://doi.org/10.1016/j.catena.2006.10.005.

Serio, M.A., Carollo, F.G., Ferro, V., 2019a. A method for evaluating rainfall kinetic power by a characteristic drop diameter. J. Hydrol. 577, 123996 https://doi.org/10.1016/j.jhydrol.2019.123996.

Serio, M.A., Carollo, F.G., Ferro, V., 2019b. Raindrop size distribution and terminal velocity for rainfall erosivity studies. A Review. J. Hydrol. 576, 210–228. https://doi.org/10.1016/j.jhydrol.2019.06.040.

Shelton, C.H., Von Bernuth, R.D., Rajbhandari, S.P., 1985. A continuous-application rainfall simulator. Transactions of the ASAE 28 (4), 1115–1119. https://doi.org/10.13031/2013.32397.

Torri, D., Regüés, D., Pellegrini, S., Bazzoffi, P., 1999. Within-storm soil surface dynamics and erosive effects of rainstorms. Catena 38 (2), 131–150. https://doi.org/10.1016/S0341-8162(99)00059-4.

Wiesner, J., 1895. Beiträge zur Kenntniss des tropischen Regens. K. Akad. Wiss., Math.-Naturw Klasse, SitzBer. 104, 1397–1434.

Wilm, H.G., 1943. The application and measurement of artificial rainfall on types FA and F infiltrometers. Eos, Trans. Am. Geophys. Un. 24 (2), 480–487. https://doi.org/10.1029/TR024i002p00480.